

Current induced torques in the presence of spin-orbit coupling

Paul M. Haney and M. D. Stiles

Center for Nanoscale Science and Technology, National Institute of Standards and Technology, Gaithersburg, Maryland 20899-6202, USA

In systems with strong spin-orbit coupling, the relationship between spin-transfer torque and the divergence of the spin current is generalized to a relation between spin transfer torques, total angular momentum current, and mechanical torques. In ferromagnetic semiconductors, where the spin-orbit coupling is large, these considerations modify the behavior of the spin transfer torques. One example is a persistent spin transfer torque in a spin valve: the spin transfer torque does not decay away from the interface, but approaches a constant value. A second example is a mechanical torque at single ferromagnetic-nonmagnetic interfaces.

Introduction— Since the prediction [1–3] of spin transfer torques in non-collinear ferromagnetic metal circuits, they have been the subject of extensive research [4, 5]. The possibility of using spin transfer torque to improve the commercial viability of magnetic random access memory (MRAM) [6], and the rich non-equilibrium physics involved establish the topic as one of practical and fundamental interest. These torques arise from the exchange interaction between non-equilibrium, current-carrying electrons and the spin-polarized electrons that make up the magnetization. In systems where the spin-orbit coupling is weak, the torque on the magnetization can be computed from the change in the spins flowing through the region containing the magnetization. This relation is a consequence of conservation of total spin. Here, we consider systems in which the spin-orbit coupling cannot be neglected (and hence total spin is no longer conserved).

In systems where spin angular momentum is not conserved, the relationship between the spin transfer torque and the flow of spins needs to be generalized. Conservation of *total* angular momentum implies that mechanical torques on the lattice of the material accompany changes in the magnetization [7, 8]. This effect has been used for decades to measure the g -factor of metals. More recent theoretical [9, 10] and experimental [11] work considers the current-induced mechanical torques present at the interface of a ferromagnet and non-magnet, similar in spirit to the spin transfer torques on the magnetization present in spin valves.

In this article we develop a theory for current induced torques (both spin transfer torques and mechanical torques) in systems with strong spin-orbit coupling, and apply it to a model of dilute magnetic semiconductors. We find that by accounting for the orbital angular momentum of the electrons, we can relate the change in total angular momentum flow to spin transfer torques and mechanical torques. We study two system geometries where these torques play important roles. The first is a spin-valve geometry, which is used to study the features of spin transfer torques in the presence of spin-orbit coupling. The second is a single interface between a ferromagnet and non-magnet, which elucidates the physics underlying current-induced mechanical torques.

Formalism — We consider a Hamiltonian consisting of a spin-independent kinetic and potential energy $\hat{H}_0 = \frac{-\hbar^2 \nabla^2}{2m} + \hat{V}(\mathbf{r})$ [12], an exchange splitting Δ , and a spin-orbit interaction parameterized by α :

$$\hat{H} = \hat{H}_0 + \frac{\Delta}{\hbar} \frac{(\mathbf{M} \cdot \hat{\mathbf{s}})}{M_s} + \frac{\alpha}{\hbar^2} (\hat{\mathbf{L}} \cdot \hat{\mathbf{s}}), \quad (1)$$

where $\hat{\mathbf{L}}$ and $\hat{\mathbf{s}}$ are the electron angular momentum and spin operators, respectively [13]. The exchange splitting arises from a magnetization \mathbf{M} , with magnitude M_s . We treat the magnetization within mean field theory.

We consider the torque on the magnetization due to electric current flow. The spin transfer torque $\boldsymbol{\tau}_{\text{STT}}$ at position \mathbf{r} from electronic states with spin density $\mathbf{s}(\mathbf{r})$ is proportional to the component of spin transfer to the magnetization [15]: $\boldsymbol{\tau}_{\text{STT}}(\mathbf{r}) = \frac{d\mathbf{M}(\mathbf{r})}{dt} = \frac{\Delta}{\hbar^2} (\mathbf{M}(\mathbf{r}) \times \mathbf{s}(\mathbf{r}))$. In the absence of spin-orbit coupling, this torque can be related to the divergence of a spin current, which offers conceptual and computational simplicity [16]. In the following we analyze how spin-orbit coupling changes this simple result.

We develop an expression for $\boldsymbol{\tau}_{\text{STT}}$ by evaluating the time-dependence of the electron spin and angular momentum densities. To do so, we adopt a Heisenberg picture of time evolution, and evaluate $\frac{d\hat{O}(\mathbf{r})}{dt} = \frac{i}{\hbar} [\hat{H}, \hat{O}^\dagger(\mathbf{r})\hat{O}(\mathbf{r})]$, where $\hat{O}(\mathbf{r})$ is the position operator, for the operators $\hat{O} = \hat{\mathbf{s}}, \hat{\mathbf{L}}$. This procedure leads to [4]:

$$\frac{d\hat{\mathbf{s}}(\mathbf{r})}{dt} = \nabla \cdot \hat{\mathbf{Q}}_s(\mathbf{r}) - \hat{\boldsymbol{\tau}}_{\text{STT}}(\mathbf{r}) + \frac{\alpha}{\hbar^2} (\hat{\mathbf{L}}(\mathbf{r}) \times \hat{\mathbf{s}}(\mathbf{r})) \quad (2)$$

where $\hat{\mathbf{Q}}_s(\mathbf{r}) = \hat{\psi}^\dagger(\mathbf{r}) \hat{\mathbf{v}} \otimes \hat{\mathbf{s}} \hat{\psi}(\mathbf{r})$, and the velocity operator is given by $\hat{\mathbf{v}} = \frac{i\hbar}{2m} (\overleftarrow{\nabla} - \overrightarrow{\nabla})$; here the arrow superscript specifies the direction in which the gradient acts. In addition:

$$\frac{d\hat{\mathbf{L}}(\mathbf{r})}{dt} = \nabla \cdot \hat{\mathbf{Q}}_L(\mathbf{r}) - \hat{\boldsymbol{\tau}}_{\text{lat}}(\mathbf{r}) + \frac{\alpha}{\hbar^2} (\hat{\mathbf{s}}(\mathbf{r}) \times \hat{\mathbf{L}}(\mathbf{r})) \quad (3)$$

where $\hat{\mathbf{Q}}_L(\mathbf{r}) = \hat{\psi}^\dagger(\mathbf{r}) \frac{1}{2} (\hat{\mathbf{v}} \hat{\mathbf{L}} + \hat{\mathbf{L}} \hat{\mathbf{v}}) \hat{\psi}(\mathbf{r})$ (the product of non-commuting operators $\hat{\mathbf{L}}$ and $\hat{\mathbf{v}}$ is symmetrized). We've defined $\hat{\boldsymbol{\tau}}_{\text{lat}}(\mathbf{r}) = \frac{i}{\hbar} \hat{\psi}^\dagger(\mathbf{r}) [\hat{H}_0, \hat{\mathbf{L}}] \hat{\psi}(\mathbf{r})$, which is

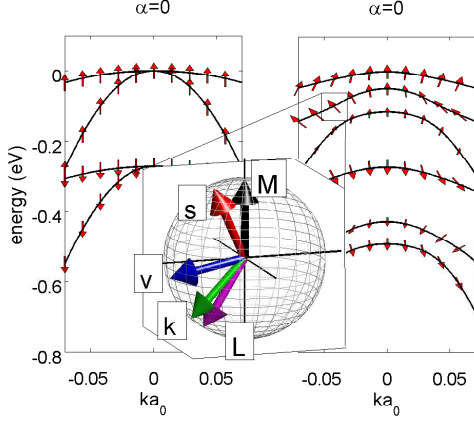


FIG. 1: Left and right panels shows GaMnAs band structure without and with spin orbit coupling, respectively (for $\gamma_2 = \gamma_3 = 2.4$). (arrows indicate spin direction of the eigenstates). The inset shows the directions of bulk magnetization, and spin, velocity, \mathbf{k} vector, and orbital moment for a single state. The torque from the misalignment between magnetization and spin, τ_{STT} , equals the torque from the misalignment between velocity and \mathbf{k} vectors, τ_{lat} .

nonzero for a potentials $V(\mathbf{r})$ which break rotational symmetry [17].

We define a total angular momentum $\hat{\mathbf{J}} = \hat{\mathbf{L}} + \hat{\mathbf{s}}$, a total angular momentum current $\hat{\mathbf{Q}}_{\mathbf{J}} = \hat{\mathbf{Q}}_{\mathbf{L}} + \hat{\mathbf{Q}}_{\mathbf{s}}$, combine Eqs. (2) and (3), and take the expectation value to obtain:

$$\frac{d\mathbf{J}(\mathbf{r})}{dt} - \nabla \cdot \mathbf{Q}_{\mathbf{J}}(\mathbf{r}) = -\tau_{\text{STT}}(\mathbf{r}) - \tau_{\text{lat}}(\mathbf{r}). \quad (4)$$

Eq. (4) is our main formal result. When spin-orbit coupling is important, the total angular momentum in the conduction electrons couples both to the magnetization and the lattice. The coupling of electron spin to the lattice requires both spin-orbit coupling and the crystal field potential. The term τ_{lat} changes the physical picture of spin transfer torque substantially, as is illustrated by a single bulk eigenstate: $\frac{d\mathbf{J}}{dt}$ and $\nabla \cdot \mathbf{Q}_{\mathbf{J}}$ vanish, however τ_{STT} and τ_{lat} may both be non-zero, implying a coupling from the angular momentum of the lattice to the magnetization (see Fig. 1). This coupling takes place through the eigenstates of the system, despite the fact that in an eigenstate, the net torque on both the spin and the orbital moment vanishes. The electronic system accommodates this coupling because the exchange torque on the spin from the magnetization is counter-balanced by a spin-orbit torque on the spin from the orbital moment. Similarly, the spin-orbit torque on the orbital moment from the spin is counter-balanced by the lattice torque on the orbital moment. Spin-orbit torque is the link between lattice angular momentum and magnetization.

Application to DMS — We apply this formalism to a model of a dilute magnetic semiconductor (DMS). DMSs

are semiconductor materials which become ferromagnetic when doped with magnetic atoms. $\text{Ga}_{1-x}\text{Mn}_x\text{As}$ is the archetype for these materials, and can be described as a system of local moments of Mn d -electrons, whose interaction is mediated by holes in the semiconductor valence band [18]. The valence states are described by the Kohn-Luttinger Hamiltonian \hat{H}_0^{KL} , which represents a small- \mathbf{k} expansion for a periodic \hat{H}_0 , acting in the $\ell = 1$ subspace (describing valence states). It is given by:

$$\hat{H}_0^{\text{KL}} = \frac{\hbar^2}{2m} \left((\gamma_1 + 4\gamma_2) k^2 - \frac{6\gamma_2}{\hbar^2} (\hat{\mathbf{L}} \cdot \mathbf{k})^2 - \frac{6}{\hbar^2} (\gamma_3 - \gamma_2) \sum_{i \neq j} k_i k_j \hat{L}_i \hat{L}_j \right), \quad (5)$$

where $\hat{\mathbf{L}}$ are the spin-1 matrices for the p -state orbitals, $\gamma_1, \gamma_2, \gamma_3$ are Luttinger parameters, and \mathbf{k} is the Bloch wave-vector. Figure 1 shows how the presence of spin-orbit coupling affects the band structure. For the results presented here, we use the default parameter values: $(\gamma_1, \gamma_2, \gamma_3) = (6.85, 2.1, 2.9)$, $\Delta = 0.27$ eV, $\alpha = 0.11$ eV. For GaAs, we set $\Delta = 0$.

For periodic systems the velocity operator can be written as: $\hat{\mathbf{v}} = \frac{1}{\hbar} \frac{\partial \hat{H}}{\partial \mathbf{k}}$, and spin and angular momentum current densities are again defined as symmetrized products of $\hat{\mathbf{v}}$ and $\hat{\mathbf{L}}$, and $\hat{\mathbf{v}}$ and $\hat{\mathbf{s}}$. The dynamics of the magnetization occur on a much longer time scale than that of the electronic states, so we compute the dynamics from a sum over scattering states, for which $\frac{ds}{dt} = \frac{d\mathbf{L}}{dt} = 0$. For the Luttinger Hamiltonian, we find the z -component of $\hat{\tau}_{\text{lat}}$:

$$\hat{\tau}_{\text{lat}}^z = (\hat{\mathbf{v}} \times \hbar \mathbf{k})_z + \frac{6(\gamma_2 - \gamma_3)}{\hbar m} \left\{ (k_x \hat{L}_y + k_y \hat{L}_x), (k_x \hat{L}_x - k_y \hat{L}_y) \right\} \quad (6)$$

where the brackets on the second term indicate an anticommutator. Other components are given by cyclic permutation of indices. In the spherical approximation ($\gamma_2 = \gamma_3$), Eq. (6) takes on a particularly simple form.

STT in spin-valves — We first consider a system to study the τ_{STT} term of Eq. (4). Figure 2(a) shows the geometry; current flows in the \hat{z} -direction, perpendicular to the magnetization of both layers. We focus on the component of torque which is in the plane spanned by the two magnetization directions. This in-plane torque is determined by the out-of-plane (or \hat{z} -component) spin density [15]. Here, $E_F = 0.16$ eV is measured from the top of the valence band. The tunnel barrier is described by Eqs. (1) and (5), with $\Delta = 0$, and with an energy offset so that the top of the valence band is 0.1 eV below E_F . We calculate the eigenstates numerically and apply boundary conditions as described in Ref. [19].

Figure 2(b) shows the spin transfer torque density as a function of distance away from the interface. We find that for $\alpha = 0$ (no spin-orbit coupling), the torque decays

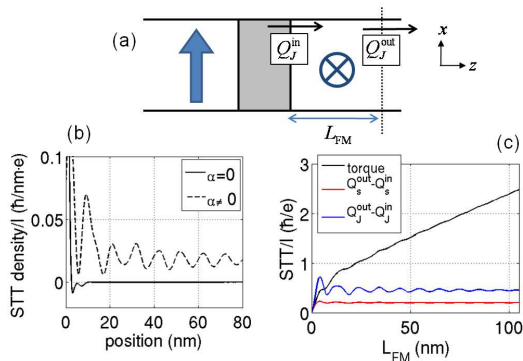


FIG. 2: Persistent spin transfer torque. Panel (a) shows the spin valve geometry treated here. The magnetizations of the ferromagnetic (FM) layers point in the \hat{x} and \hat{y} (out-of-page) directions. Panel (b) shows the spin transfer torque density as a function of distance away from the right tunnel barrier-FM interface with and without spin-orbit coupling. This torque density decays to zero in the absence of spin-orbit coupling, while it oscillates around a finite value in the presence of spin-orbit coupling. Panel (c) shows the total spin transfer torque, the net flux of spin current, and net flux of total angular momentum current versus FM thickness. The change in the spin and angular momentum currents approaches a finite value, while the total torque does not. The linear dependence for large thickness indicates a persistent spin transfer torque density due to coupling to the lattice angular momentum.

to zero away from the interface, as expected [16]. For $\alpha \neq 0$, the torque oscillates around a nonzero value, and extends into the bulk. Figure 2(c) shows that the total spin transfer torque as a function of ferromagnetic layer thickness L_{FM} is proportional to thickness for large L_{FM} . This is in contrast to the metallic spin valve, where the torque is an interface effect and becomes constant for large L_{FM} .

This persistent spin transfer torque arises because the spins of individual eigenstates are not aligned with the magnetization (see Fig. 1) in the presence of spin-orbit coupling. The misalignment gives rise to a torque between the lattice and the magnetization. In equilibrium, these torques cancel when summed over all occupied states. However, the presence of a current changes the occupation of the bulk states possibly eliminating the cancellation. In systems without inversion symmetry, this mechanism causes spin transfer torque even in single domain bulk ferromagnets [20, 21]. In bulk GaMnAs however, inversion symmetry is only very weakly broken, and the standard Kohn Luttinger Hamiltonian, Eq. (5) treats the system as inversion symmetric. In the system we consider, the interfaces between dissimilar materials break inversion symmetry, enabling the

scattering (not included here). For materials that strongly break inversion symmetry, unlike GaMnAs, even scattering would not eliminate the persistent transverse

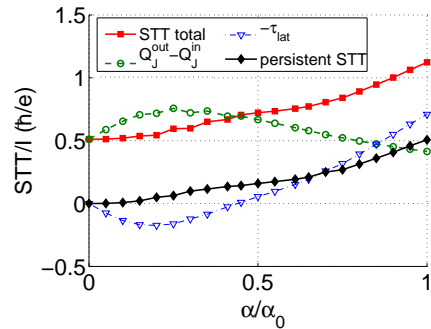


FIG. 3: The total spin transfer torque, the net flux of total angular momentum, and the persistent component of the spin transfer torque as α is increased from 0 to $\alpha_0 = 0.11$ eV.

spin accumulation [20, 21]. We note that strain can also break inversion symmetry in GaMnAs, enabling the observation of persistent spin transfer torque in a single ferromagnetic layer [22, 23]. In our results, the coherence between the states modifies the spin accumulation and the torque near the interface but these corrections decay away from the interface due to dephasing.

Figure 3 shows, as a function of the spin orbit coupling constant α , the values of total spin transfer torque, the angular momentum current flux, the lattice torque, and the persistent contribution to spin transfer torque (for $L_{\text{FM}} = 30$ nm). We determine the persistent contribution from the slope of the integrated total versus FM width L_{FM} at large L_{FM} (see Fig. 2c). In this example, the spin transfer torque increases with the addition of spin-orbit coupling, largely because of the addition of the persistent term. This qualitative behavior depends on system parameters: for $E_{\text{F}} = 0.34$ eV, for example, the spin-orbit coupling decreases the total torque. For the layer thicknesses considered here, the angular dependence of the torques is similar that of metallic systems. Both the total and persistent spin transfer torques vanish for collinear configurations and are roughly sinusoidal for intermediate angles.

Nanomechanical torques in wires — We next consider a system with a single interface between GaMnAs and GaAs, with the direction of the magnetization parallel to the current flow. This is similar to the geometry considered in previous theoretical and experimental work [9–11] on the coupling of spin current to a lattice torque. Here, we show that this can come from the spin-orbit coupling in the band structure in addition to spin flip scattering treated previously [9–11]. We use the same parameters as before, except $E_{\text{F}} = 0.06$ eV, and the top of the valence band of both layers coincide.

Our calculation shows that as a function of distance away from the interface the torque from a particular channel oscillates, while the total torque shows oscilla-

tory decay. The oscillatory decay can be understood similarly to the oscillatory decay of the spin transfer torque in ferromagnets without spin-orbit coupling. For a coherent interface, each incident state from the GaMnAs with particular a k_x , k_y transmits into the available channels of GaAs at that transverse wave vector and energy. These different channels have different \mathbf{J} character and wave vector k_z . They interfere with each other, leading to an oscillatory $\mathbf{J}(z)$, with an oscillation period inversely proportional to the splitting of k_z wave-vectors of the different sheets of the Fermi surface. This splitting is from the lattice crystal field and spin-orbit coupling, the agents responsible for $\boldsymbol{\tau}_{\text{lat}}$. Different channels have different oscillation periods, so that their sum decays away from the interface, as happens for spin transfer torques in ferromagnets [16].

For the parameters used here, we find the angular momentum current of the states entering the system from the GaMnAs is $Q_{J_z}^{\text{in}} = 1.09\hbar \frac{I}{e}$, while that persisting to the end of the GaAs is $Q_{J_z}^{\text{out}} = 0.46\hbar \frac{I}{e}$. We calculate the mechanical torque to be $0.63\hbar \frac{I}{e}$, which is equal to the difference between the incoming and outgoing angular momentum currents for this particular system. For appropriate experimental conditions, this torque is greater than the thermal fluctuations and is a measurable effect. We refer the reader to Ref. [9–11] for details of treatment of the torsion dynamics and experimental details.

The formalism developed here generalizes previous

work to allow for the microscopic evaluation of the electronic structure contribution to the current-induced mechanical torque. For systems with nonzero magnetization, the microscopic form of $\boldsymbol{\tau}_{\text{lat}}$ is necessary to determine the partitioning of total angular momentum flux between torques on the magnetization and torques on the lattice. Our theory neglects other mechanisms of spin relaxation, such as disorder-induced spin-flip scattering, so that full calculations will require microscopic calculations like these to be embedded in diffusive transport calculations.

Conclusion— We have shown how atomic-like spin-orbit coupling affects current-induced torques: both the spin transfer torque on the magnetization and the mechanical torque on the lattice. In GaMnAs spin valves, we find a contribution to the spin transfer torque that persists throughout the bulk. This result may explain experiments which find critical currents which are up to an order of magnitude smaller than the value expected from a simple accounting of the net spin current flux [24, 25]. For a single interface between GaMnAs and GaAs, we microscopically compute the mechanical torque due to scattering from the interface. These results highlight important, qualitatively different physics at play when spin-orbit coupling is strong.

The authors acknowledge helpful conversations with A. H. MacDonald.

-
- [1] L. Berger, J. Appl. Phys. **3**, 2156 (1978); *ibid.* **3**, 2137 (1979).
 - [2] J. Slonczewski, J. Magn. Magn. Mat. **62**, 123, (1996).
 - [3] L. Berger, Phys. Rev. B **54**, 9353 (1996).
 - [4] D. C. Ralph and M. D. Stiles, J. Magn. Magn. Mater. **320**, 1190 (2007).
 - [5] M. D. Stiles and J. Miltat, Top. Appl. Phys. **101**, 225 (2006).
 - [6] J. A. Katine and E. E. Fullerton, J. Magn. Magn. Mater. **320**, 1217 (2007).
 - [7] O. W. Richardson, Phys. Rev. **26**, 248 (1908).
 - [8] A. Einstein and A. de Hass, Verhandlungen der Deutschen Physikalischen Gesellschaft, **17**, 152 (1915).
 - [9] P. Mohanty *et al.*, Phys. Rev. B **70**, 195301 (2004).
 - [10] A. A. Kovalev *et al.*, Phys. Rev. B **75**, 014430 (2007).
 - [11] G. Zolfagharkhani *et al.*, Nature Nanotech. **3**, 720 (2008).
 - [12] We neglect phonon scattering in this paper. It may be included by the addition of the phonon Hamiltonian and phonon-electron coupling to H_0 .
 - [13] There are two contributions to the orbital moment, an atomic-like contribution and a contribution to the total orbital angular momentum from itinerant motion through the lattice. If we assume that the atomic-like contribution dominates the coupling to the spin, the itinerant contribution drops out of the problem. Such approximations are generally quite good because spin-orbit coupling is strongest in the atomic core regions due to the large electric field. The distinction between “local” and “itinerant” orbital angular momentum is discussed in Ref. [14].
 - [14] T. Thonhauser *et al.*, Phys. Rev. Lett. **95**, 137205 (2005).
 - [15] A. S. Núñez and A. H. MacDonald, Solid State. Comm. **139**, 31 (2006).
 - [16] M. D. Stiles and A. Zangwill, Phys. Rev. B **66**, 014407 (2002).
 - [17] In deriving Eqs. (3), the commutator of the kinetic energy operator with the position operator $\hat{\psi}$ gives the divergence of the angular momentum current. For $H_0 = -\hbar^2 \nabla^2 / 2m + V(\mathbf{r})$, our definition of $\hat{\mathbf{n}}_{\text{at}}$ is equivalent to $[V(\mathbf{r}), \hat{\mathbf{L}}]$ because the kinetic energy commutes with the rotation operator.
 - [18] T. Jungwirth *et al.*, Rev. Mod. Phys. **78**, 809 (2006).
 - [19] A. M. Malik *et al.*, Phys. Rev. B **59**, 2861 (1998).
 - [20] A. Manchon and S. Zhang, Phys. Rev. B **78**, 212405 (2008).
 - [21] Ion Garate and A. H. MacDonald, Phys. Rev. B **80**, 134403 (2009).
 - [22] A. Chernyshov, *et al.*, Nat. Phys. **5**, 656 (2009).
 - [23] K. M. D. Hals *et al.*, Euro. Phys. Lett. **90**, 47002 (2010).
 - [24] D. Chiba *et al.*, Phys. Rev. Lett. **93**, 216602 (2004).
 - [25] M. Elsen *et al.*, Phys. Rev. B **73**, 035303 (2006).